Proceedings of IMECE 2008
2008 ASME International Mechanical Engineering Congress and Exposition
November 2-6, 2008, Boston, Massachusetts, USA

IMECE2008-68860

THERMOELECTRIC HEAT RECOVERY FROM A TANKLESS WATER HEATING SYSTEM

S. A. LeBlanc
Stanford University
Stanford, California, USA

Y. Gao
Stanford University
Stanford, California, USA

K.E. Goodson
Stanford University
Stanford, California, USA

ABSTRACT

Thermoelectric cogeneration promises to recover waste heat energy from a variety of combustion systems. There is a need for computationally efficient simulations of practical systems that allow optimization and illustrate the impact of key material and system parameters. Previous research investigated thermoelectric material enhancement and thermoelectric system integration separately. This work connects material parameters and system integration. We develop a thermal simulation for a 15kW tankless, methane-fueled water heater with thermoelectric modules embedded within a cross-flow heat exchanger. The simulation employs a finite volume method for the two fluids. It links external convection with a surface efficiency of 85%, internal convection for laminar flow, and conduction through the system in order to determine power generation within the thermoelectric. For a single pipe in the water heater system, 126 W of electrical power can be generated, and a typical system could yield 370 W. Realization of effective cogeneration systems hinges on investigating the impact of thermoelectric material parameters coupled with system parameters, so the impact of varying flow rate, convection coefficient, TEM thermal conductivity, Seebeck coefficient, and thermal interface materials are investigated. While varying parameters can improve thermoelectric output by over 50%, thermal interface materials can severely limit cogeneration system power output.

INTRODUCTION

The inefficiency of energy systems is due largely to thermal losses [1]. Thermoelectric modules (TEMs) operating as generators can improve efficiency because they utilize the temperature gradients in energy systems to convert heat energy to electrical energy. TEMs used in this way are often called thermoelectric generators (TEGs). TEGs are attractive cogeneration solutions because they are reliable, silent, and have no moving parts. Moreover, they offer the benefit of distributed electricity generation where electricity is generated at the required location rather than obtained from a distant power plant. Since the cost to deliver electricity is expected to increase more than electricity demand [2], TEGs can be particularly advantageous in systems such as automobiles, electronics, and appliances which are used by individuals or small groups. Extensive effort has been focused on utilizing waste heat for thermoelectric energy conversion [3-5]. However, TEGs can also be used in systems such as water heaters in which the goal is to transfer heat energy [6].

Previous work can be separated into two general areas, thermoelectric materials and systems with incorporated TEMs. System-level characterization and modeling provided a proof of concept and initial estimates of TEM performance. TEGs incorporated with heat exchangers in combustion systems demonstrated promising electrical power generation [3-5, 7]. A major challenge with system development is inefficiency due to thermal interface resistances [8]. Wide temperature fluctuations, prolonged thermal cycling, and large contact area in thermoelectric systems both degrade the performance of traditional thermal interface materials (TIMs) and make the module more susceptible to device failure from thermal expansion mismatch [9]. Possible damage from thermal expansion also limits the rate of temperature change in a TEM [10]. Nano-structured thermal interfaces composed of carbon nanotubes (CNTs) are aptly suited for thermoelectric applications. Previous work has shown that CNT arrays may perform as an exceptional thermal interface material because they have both high thermal conductivity and mechanical compliance [11, 12].

There is a distinction between maximizing a thermoelectric material's efficiency and maximizing the output of a TEG integrated into a system [13]. Much research has focused on improving TEM performance through the figure of merit of thermoelectric materials, $Z = S^2/\rho k$, where S, ρ, and k are the Seebeck coefficient, electrical resistivity, and thermal

conductivity of the thermoelectric material, respectively. This figure is often multiplied by the average temperature within the TEM and reported as *ZT*. There has been considerable effort to develop phonon-glass/electron-crystal materials to reduce thermal conductivity. Groups have investigated controlling the crystal structure of bulk thermoelectric materials as well as developing nano-structured materials to increase phonon scattering and improve the thermoelectric figure of merit [14]. However, maximizing *Z* is not necessarily the optimal method to optimize an entire cogeneration system [15], and the latter is of practical concern. For example, combustion systems and robust electronic systems experience high operating temperatures and large temperature fluctuations, but the efficiency of many thermoelectric materials rapidly declines at high temperatures. Hence, it is essential to consider the TEM efficiency required for a given application in order to select an appropriate material. The realization of practical, effective cogeneration systems hinges on investigating the impact of thermoelectric material parameters coupled with system parameters.

The current work simulates a 15 kW, methane-fueled, tankless water heater. Also termed demand or instantaneous water heaters, tankless water heaters use a heat source to directly heat cold water without storing water in a tank and incurring energy loss [16-18]. The large temperature gradient between the heat source and the cold water is ideal for thermoelectric cogeneration. This work is unique in that it investigates TEM output when both material properties and system parameters are considered. We not only investigate varying thermal interface materials, but we present the potential of a TIM made with a CNT array. By simulating a TEM integrated into a tankless water heater, we are able to demonstrate limiting thermal resistances in a thermoelectric cogeneration system and inform system optimization by varying parameters.

NOMENCLATURE

A	heat transfer area [m^2]
h_g	gas stream convection coefficient [W/m^{2}K]
h_w	water stream convection coefficient [W/m^{2}K]
I	current [A]
k, k_{TEM}	thermal conductivity of TEM material [W/m$^-$K]
P	electrical power from TEM [W]
q_g	heat transfer rate from gas stream [W]
q_{Joule}	Joule heating [W]
$q_{Peltier}$	heat transfer due to Peltier effect [W]
q_{TEM}	heat transfer rate through TEM [W]
q_w	heat transfer rate to water stream [W]
R_{load}	electrical resistance of load [Ω]
R_{pw}	conduction resistance of pipe wall [K/W]
$R_{TEM,e}$	electrical resistance of TEM [Ω]
S	Seebeck coefficient [V/K]
$T_{g,i}$	gas inlet temperature [K]
$T_{g,o}$	gas outlet temperature [K]
T_p	exterior pipe wall temperature [K]
T_{pw}	interior pipe wall temperature [K]
t_{TEM}	TEM thickness [m]
$T_{TEM,c}$	TEM cold side temperature [K]
$T_{TEM,h}$	TEM hot side temperature [K]
T_w	water temperature [K]
Z	thermoelectric figure of merit [1/K]

Greek symbols

ΔT_{lm}	log mean temperature difference [K]
ΔT_{TEM}	temperature difference across TEM [K]
ρ	electrical resistivity [Ω-m]
η_o	total fin surface efficiency

SIMULATION

A tankless water heater system is simulated numerically. This practical heat exchanger setup is used in many applications in which cogeneration may be feasible. Figure 1a shows the fluid cross-flow arrangement through an annular-finned pipe. A water heater system has multiple pipes like the one shown. The thermoelectric module is modeled as a ring-shaped structure to match the pipe's shape [19]. The TE material is surrounded by an electrical conductor, a ceramic insulating layer, and a thermal interface material to connect the TEM to the pipe. Figure 2 provides a thermal circuit model for the system including the temperatures of the hot gas stream and the water stream as nodes. The model accounts for external gas convection, heat generation by the TEM, and the flow rate dependence of the convection coefficients.

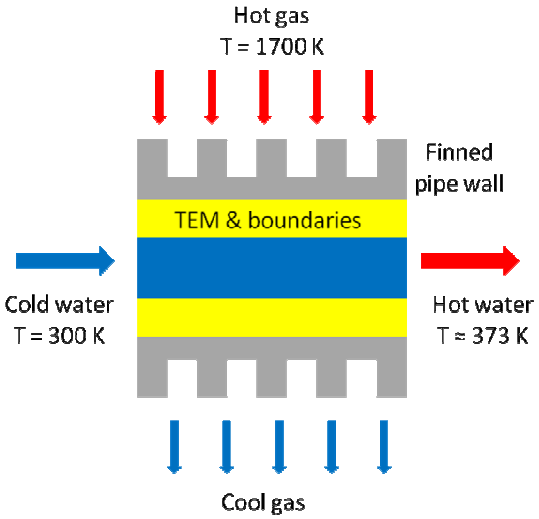

(a)

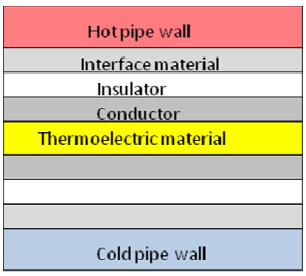

(b)

Figure 1. a) Cross-sectional view of finned pipe in a water heater system. The pipe length, inner diameter, and outer fin diameter are 300 mm, 30 mm, and 60 mm, respectively. b) Boundary materials surrounding the thermoelectric material.

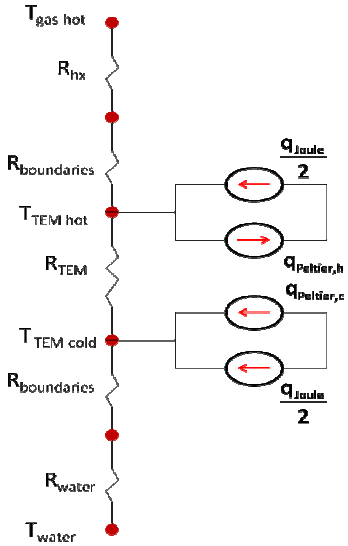

Figure 2. Thermal circuit of transverse (gas flow) direction. The boundaries include conductor, insulator, and thermal interface material.

The external and internal convection components use empirical correlations to determine the average convection coefficients. The heat transfer from the gas stream is determined using

$$q_g = \left[\frac{1}{\eta_o h_g A} + R_{pw} \right]^{-1} \Delta T_{lm} \qquad (1)$$

This accounts for the effective fin efficiency of the annular pipe wall fins through η_o and the cylindrical wall conduction resistance [20]. The average gas convection coefficient is determined from a correlation for a compact heat exchanger with circular finned pipes by Jameson [21]. The driving temperature difference between the gas and the pipe is approximated using a log mean temperature relationship.

$$\Delta T_{lm} = \frac{\left(T_{g,o} - T_p\right) - \left(T_{g,i} - T_p\right)}{\ln\left(\frac{T_{g,o} - T_p}{T_{g,i} - T_p}\right)} \qquad (2)$$

Integrating the differential heat transfer between two fluids over an exchange area in a heat exchanger leads to a logarithmic relationship between the temperature differences. Modeling the temperature gradient this way allows a close approximation of the pipe wall temperature and its variation in the water flow direction without requiring a detailed solution of the temperature profile in the pipe wall along the gas flow direction. The heat transfer from the interior pipe wall to the water stream is

$$q_w = h_w A\left(T_{pw} - T_w\right) \qquad (3)$$

and h_w is determined from the correlation for laminar internal flow of Sieder and Tate [20].

As indicated in Figure 2, the heat transfer through the TEM must account for Joule heating and the Peltier effect in addition to conduction through the TEM. The Peltier heat flux is dependent on the temperature of each side of the TEM.

$$q_{TEM} = \frac{k_{TEM}\left(T_{TEM,h} - T_{TEM,c}\right)}{t_{TEM}} \qquad (4)$$

$$q_{Joule} = I^2 R_{TEM,e} \qquad q_{Peltier} = S T_{TEM,h,c} I \qquad (5,6)$$

The temperature gradient through the TEM determines the electrical potential developed across the TEM. The electrical power obtained from the TEM once it is connected to a load resistor is

$$P = I^2 R_{load} = I(S\Delta T_{TEM} - I R_{TEM,e}) \qquad (7)$$

where the product of the Seebeck coefficient and the temperature difference is the voltage drop developed. In the simulation of the water heater system, the temperature range around the TEM is 400 K to 600 K. The performance of thermoelectric materials is temperature dependent. The compound PbTe is an optimal thermoelectric material at these operating temperatures, so the properties of PbTe are used initially for the simulation [22]. Thermal and electrical interface resistances are at first neglected to ascertain upper bounds. Varying thermoelectric material properties and thermal interface materials are considered.

The simulation of a heat exchanger with an integrated TEM is conducted using a finite volume method. Each pipe is discretized in the longitudinal direction. A shooting method is used to determine the water temperature for each volume. The water temperature is assumed to be a mixed mean temperature that represents the entire discrete volume. A false position or regula falsi method allows convergence on the amount of heat transferred to the water. This simulation approach is simpler than a finite element model, and it captures the significant thermal and electrical physics of the system. The approach enables the revelation of key parameters and their relative significance in system optimization.

RESULTS AND DISCUSSION

Two key findings result from simulating a TEM integrated into a cross-flow heat exchanger. First, system optimization relies on strategically enhancing certain system and TEM parameters. The impacts of varying fluid flow rates, TEM thickness, thermoelectric material thermal conductivity, and Seebeck coefficient are investigated. Second, the thermal resistances of system components surrounding the TEM limit TEM output power. The effects of standard interface materials and a novel CNT material are compared in the water heater simulation.

In order to isolate the influence of system and TEM parameters, a single pipe of a tankless water heater system is simulated initially. Figure 3 summarizes a single pipe simulation. In Figure 3a, the change in fluid temperatures demonstrates energy exchange between the hot gas and the water. With the selected system specifications, the gas and the water do not reach the same temperature before the water exits the pipe. In the cases of longer pipe length or lower water flow rate, a decrease in the rate of change in temperature with distance is evident. The temperature drop across the TEM along the length of the pipe decreases, so the voltage developed across the TEM diminishes. In optimizing a system, the change in temperature drop may indicate that thermoelectric material could vary along the length of the pipe since the thermoelectric figure of merit *ZT* is temperature dependent.

Figure 3b depicts the total electrical power from the TEM as a function of current through the TEM. Current and load resistance are inversely related, so increasing current corresponds to decreasing load resistance. As expected, the peak power output occurs where the load resistance is equal to the electrical resistance of the TEM. The average gas outlet temperature declines as more heat energy is converted to electrical energy. The water outlet temperature changes minimally because the heat capacity rate, the product of mass flow rate and specific heat capacity, is larger for the water stream than the gas stream. The ability to obtain the maximum electrical power out without significantly reducing the water output temperature is promising.

The relative change in power as load resistance decreases is also noteworthy. The electrical power from the TEM can be divided by the energy transferred into the system from the hot gas minus the amount of energy transferred to the water to obtain a non-dimensional power value. For a single pipe, this non-dimensional power peaks at 0.8% with an average gas outlet temperature of 1100 K indicating a significant amount of energy that can still be harvested from the gas. The voltage developed across the TEM is dropped across the TEM electrical resistance and an external load resistance. While the electrical power output comes from the voltage drop across the load resistor, the power dissipated in the TEM contributes to Joule heating and can be beneficial in this system to heat the water. The electrical power output is 43 times larger than the power dissipated in the TEM at low current (high load resistance) values. The ratio of electrical power output to power dissipated decreases from an initial amount of 21 per Ampere to 1per Ampere at the matched load condition. This corresponds to an initial incremental increase in electrical power of 6.8 W/A, and the increase in power per unit rise in current declines to zero at 37 A. Because the increase in incremental TEM output power diminishes, the optimal operating point may not be at the peak power condition.

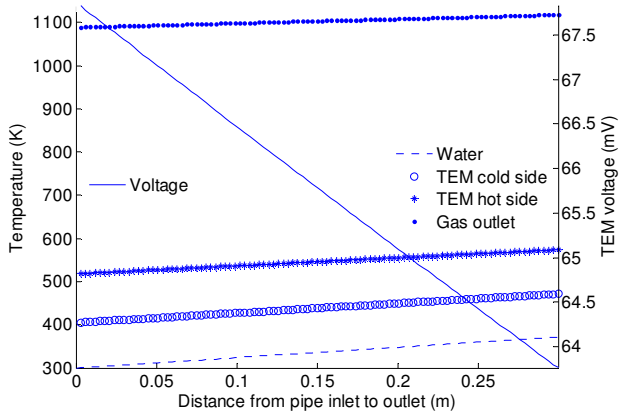

(a)

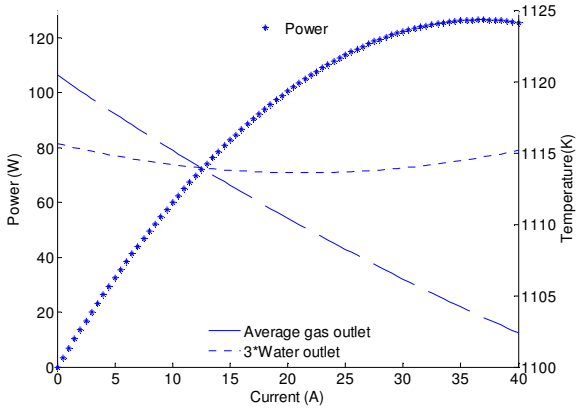

(b)

Figure 3. a) Fluid temperatures, TEM boundary temperatures and TEM voltage as a function of distance along the pipe b) Electrical power output from TEM and resulting change in gas and water outlet temperatures. Water temperature has been rounded to the nearest Kelvin. The maximum power output for the simulated heat exchanger is 126 W.

The relative influence of system and TEM parameters informs the optimization of a thermoelectric cogeneration system, so we determine the impact of varying parameters. As seen in Figure 4, the thermoelectric power output rises at a declining rate as the flow rate of the water stream increases. The rise is due to increased convective cooling of the pipe wall resulting in a larger temperature drop across the TEM. The relative impact of reducing the thermal convection resistance decreases, and the energy transfer within the water dominates.

Modifying the gas convection coefficient h_g mimics multiple system variations. For example, altering fin geometry or gas flow rate will change h_g. Moreover, there is uncertainty around the value of h_g because it is highly dependent on flow properties and system geometry, and the empirical correlation used is only the best available approximation to the geometry considered. Figure 5 shows the benefit of improving the convection coefficient; doubling the convection coefficient can increase the electrical power output by 50%. Additionally, the value of h_g affects the impact of the gas side convective thermal resistance relative to the other system thermal resistances. Crane indicated the importance of convective resistance but indicated that it is often the highest heat transfer resistance [5]. Our results indicate that the gas side convective resistance can be comparable to TEM resistance as TEM thickness increases. The relative importance of interface resistance increases as the gas side convection improves. The limiting effect of interface materials is discussed in more detail at the end of this section.

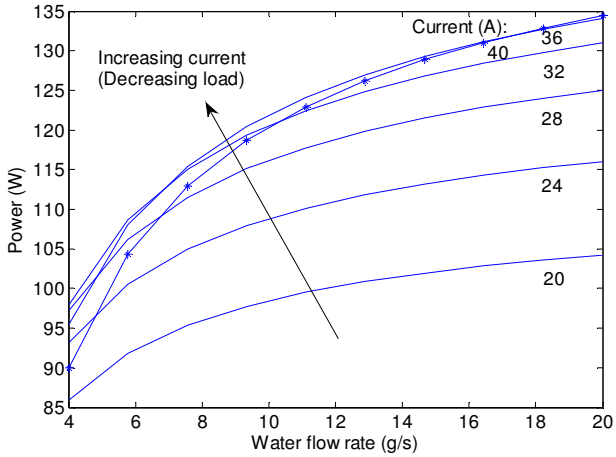

Figure 4. TEM electrical power output for increasing water mass flow rates at increasing values of current through the TEM. For load resistances less than the TEM electrical resistance, output power decreases.

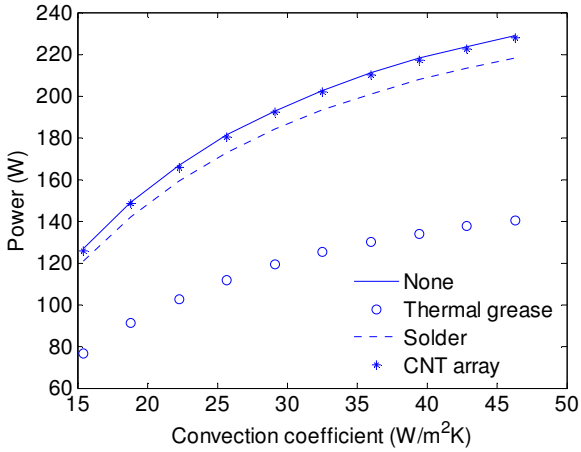

Figure 5. TEM electrical power output for increasing gas convection coefficient and varying interface materials.

The impact of TEM parameters such as thermal conductivity, Seebeck coefficient, and TEM thickness is depicted in Figure 6-Figure 8. Figure 6 demonstrates that a 100 μV/K increase in Seebeck coefficient augments the power by 19 W. The top axis shows the *ZT* corresponding to each Seebeck coefficient value. All other properties are held constant. The temperature for the *ZT* computation is the average temperature across the TEM. The *ZT* value indicates the material parameter required. A PbTe material would have a *ZT* of approximately 1.7 for the water heater operating system. The maximum operating temperature of the thermoelectric material must be considered in evaluating the ZT. For example, Bi_2Te_3 has a maximum operating temperature of about 550 K and could not be considered for this application.

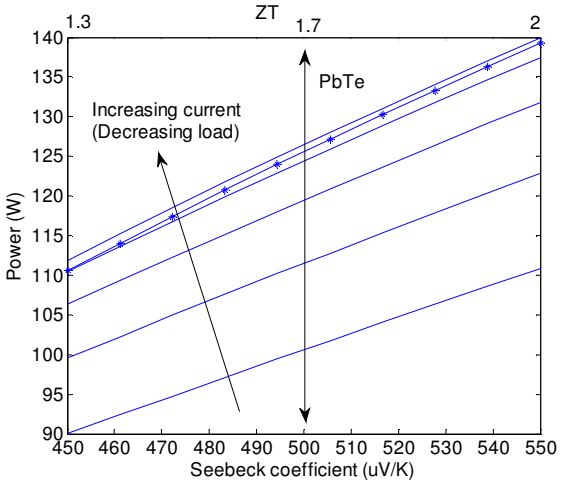

Figure 6. TEM electrical power output as a function of Seebeck coefficient and decreasing load resistance. The '*' shows where the load resistance decreased below the TEM resistance. The top axis shows the corresponding ZT where T is taken at the average temperature across the TEM at 30 A.

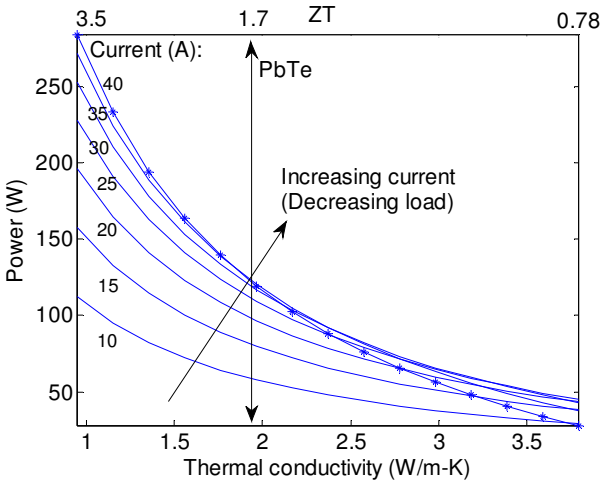

Figure 7. TEM electrical power output for thermoelectric material conductivities as low as 1 W/m-K. The ZT indicates that operating temperature is much higher than typical thermoelectric applications, and TEM material selection must account for this.

Altering the TE thermal conductivity as opposed to the Seebeck coefficient is more effective as shown in Figure 7. The output power is more than doubled if the thermal conductivity is reduced by 1 W/m-K. Of all the parameters considered, thermal conductivity improvement results in the largest gain in power output.

In addition to thermoelectric material properties, we consider the impact of TEM thickness and the interface around the TEM. These two parameters are closely related because the interface resistance degrades system efficiency at a rate that depends strongly on thermoelectric thickness. Figure 8 illustrates that a thicker TEM raises the TEM thermal resistance and thus the temperature drop across the TEM. Hence, a 22 W/mm improvement in power is possible. The thermal interface material strongly reduces the output power and severely affects power output as TEM thickness increases.

Estimating the thermal resistance of interface materials is a major challenge for this work. Interface materials from thermal greases to metallic alloys have thermal conductivities ranging from 0.2 to 50 W/m-K [23]. In modern computers, these materials have thicknesses between 20 and 100 µm, yielding total thermal resistances from 150 to 0.6 m^2K/MW. In macroscale systems such as a water heater the thicknesses of interface materials can be substantially larger. The large thickness is owed to geometrical inconsistencies in the larger components as well as the requirement for the interface to overcome thermomechanical mismatch between the adjacent materials. In contrast to computers, which are subjected to a temperature variation of approximately 100 K, combustion-based TEM systems could experience thermomechanical cycling up to 600 K. For the present work, we assume a TIM thickness of 1 mm and thermal conductivities of 1 W/m-K for grease, 10 W/m-K for metal solder, and 100 W/m-K for a novel CNT-based interface material [12].

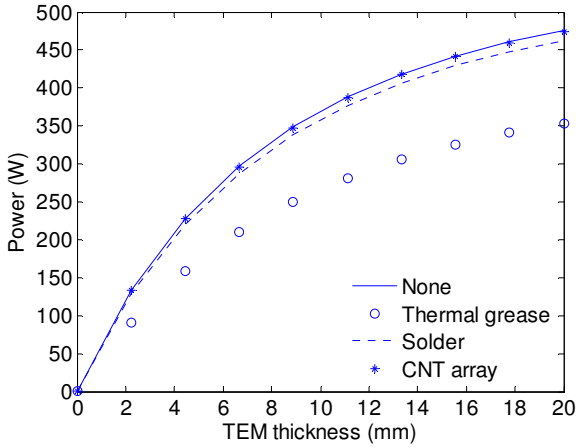

Figure 8. TEM electrical power output as a function of TEM thickness and interface material. For these calculations, an interface materal thickness of 1 mm is used.

The maximum electrical power output depends on the configuration of the heat exchanger system. Options for pipe configurations in the water heat system are considered in Table 1. The table provides the incremental gain in adding pipes in multiple configurations. Pipes located next to each other horizontally are in a parallel thermal connection whereas vertically stacked pipes are in a series thermal connection. The gas outlet temperature is indicative of the amount of energy remaining in the gas stream after it has passed over all of the pipes. Because the gas stream temperature drops as it passes over the pipes, the electrical power out of a pipe's TEM decreases as it is stacked lower in a vertical arrangement. However, increasing the number of pipes stacked horizontally would also require an increase in the mass flow rate of the gas stream. Additionally, the average temperature across the TEM is significantly different in each pipe, so different thermoelectric materials should be considered. The TEM material in each pipe should have a peak *ZT* for the operating temperature of that pipe. The incremental gain in power as a function of pipe configuration should be considered along with the maximum possible power output.

Table 1. Configurations of pipes connected thermally in parallel and series. TEM electrical output increases most for parallel arrangements at the cost of higher gas flow rates.

Pipe configuration	Diagram of cross-section	Peak power output (W)	Gas outlet temp. (K)	Thermal connection
Single		250	1100	
4 horizontal, stacked		340	740	2 parallel sets with 2 in series
6 horizontal, stacked		370	530	3 parallel sets with 3 in series
4 horizontal *requires higher gas flow rate		500	1100	4 in parallel

CONCLUSION

A tankless water heater system with an integrated thermoelectric module is simulated numerically. The impact of varying both system and TEM parameters is determined. The most effective way to increase electrical power output from the TEM is to reduce the TEM thermal conductivity; reducing the thermal conductivity by 50% can double the power output. Increasing the hot side convection coefficient and increasing the TEM thickness can increase the output power by up to 50%.

Thermal interface materials significantly limit the ability of a TEM to maximize output in a cogeneration system. We demonstrate that industry standard TIMs can reduce TEM power output by approximately 40% depending on material and thickness. More work is needed to minimize this thermal resistance while accounting for the severe repetitive thermomechanical cycling in these systems. In any case, the current work suggests that novel interfaces such as those based on CNT technology are encouraging options for future research.

Thermoelectrics offer a promising cogeneration opportunity, and enhancements in TEM materials will improve the technology's potential. Recognizing and solving the remaining challenges of TEM system integration are required to improve overall system efficiency and power output.

ACKNOWLEDGMENTS

Discussions with Drs. Sungbae Park and Daehyun Wee of Bosch Research Corporation were very helpful in completing this work. We also acknowledge the support of the National Science Foundation Graduate Research Fellowships.

REFERENCES

[1] "World Energy Outlook," *International Energy Agency,* 2002.

[2] E. I. Administration, "Short Term Energy Outlook," D. o. Energy, Ed., 2008.

[3] E. F. Thacher, B. T. Helenbrook, and C. J. Richter, "Testing of an automobile exhaust thermoelectric generator in a light truck," *Proceedings of IMECHE,* vol. 221, 2007.

[4] K. Nagao, A. Nagai, I. Fujii, T. Sakurai, M. Fujimoto, T. Furue, T. Hayashida, Y. Imaizumi, and T. Inoue, "Design of Thermoelectric Generation System Utilizing The Exhaust Gas of Internal-Combustion Power Plant," *17th International Conference on Thermoelectrics,* 1998.

[5] D. T. Crane and G. S. Jackson, "Optimization of cross flow heat exchangers for thermoelectric waste heat recovery," *Energy Conversion and Management,* vol. 45, pp. 1565-1582, 2004.

[6] M. D. Rowe, G. Min, S. G. K. Williams, A. Aoune, K. Matsuura, V. L. Kznetsov, and L. W. Fu, "Thermoelectric recovery of waste heat - case studies," *Proceedings of the Thirty-Second Intersociety Energy Conversion Engineering Conference,* vol. 2, July 1997 1997.

[7] J. Vazquez, Miguel A. Sanz-Bobi, Rafael Palacios, Antonio Arenas, "State of the Art of Thermoelectric Generators Based on Heat Recovered from the Exhaust Gases of Automobiles."

[8] A. M. Pettes, M. S. Hodes, and K. E. Goodson, "Optimized Thermoelectric Refrigeration in the Presence of Thermal Boundary Resistance," *Proceedings of IPACK2007,* July 8-12, 2007 2007.

[9] F. Co., "Thermoelectric Technical Reference: Reliability of Thermoelectic Coolers," 2008.

[10] B. Yang, "Thermoelectric Technology Assessment," in *ARTI Research Program*: Air-Conditioning and Refrigeration Technology Institute, Inc., 2007.

[11] T. Tong, Z. Yang, L. Delzeit, A. Kashani, M. Meyyappan, and A. Majumdar, "Dense Vertically Aligned Multiwalled Carbon Nanotube Arrays as Thermal Interface Materials," *Components and Packaging Technologies, IEEE Transactions on,* vol. 30, pp. 92-100, 2007.

[12] M. Panzer, G. Zhang, D. Mann, X. Hu, E. Pop, H. Dai, and K. E. Goodson, "Thermal Properties of Metal-coated Vertically-Aligned Single-Wall Nanotube Arrays," *Journal of Heat Transfer,* 2007 2007.

[13] G. J. Snyder and E. S. Toberer, "Complex thermoelectric materials," *Nature Materials,* vol. 7, February 2008 2008.

[14] G. S. Nolas, J. Poon, and M. Kanatzidis, "Recent Developments in Bulk Thermoelectric Materials," *MRS Bulletin,* vol. 31, March 2006 2006.

[15] M. Chen, L. Shan-Shan, and B. Liao, "On the Figure of Merit of Thermoelectric Generators," *Journal of Energy Resources Technology,* vol. 127, p. 5, March 2005 2005.

[16] "A Consumer's Guide to Energy Efficiency and Renewable Energy," U. S. D. o. Energy, Ed., 2005.

[17] "http://www.boschhotwater.com/."

[18] N. Kloub, "Improving the Gas Instantaneous Water Heaters Performances," *American Journal of Applied Sciences,* vol. 2, pp. 1008-1013, 2005 2005.

[19] G. a. D. M. R. Min, "Ring-structured thermoelectric module," *Semiconductor Science and Technology,* vol. 22, p. 4, 2007 2007.

[20] F. P. Incropera, *Fundamentals of Mass and Heat Transfer*. New York: McGraw-Hill, 2007.

[21] W. M. Kays and A. L. London, *Compact Heat Exchangers*. New York: McGraw-Hill, 1984.

[22] *CRC handbook of thermoelectrics*. Boca Raton: CRC Press, 1995.

[23] R. Prasher, "Thermal interface materials: Historical perspective, status, and future directions," *Proceedings of the IEEE,* vol. 94, pp. p.1571-1586, August 2006 2006.